Key Points:
- We propose that horse-collar auroras, which occur during prolonged periods of northward IMF, are a signature of dual-lobe reconnection
- The dayside polar cap is eroded and replaced by magnetic flux newly closed by dual-lobe reconnection, filled with sun-aligned arcs
- We discuss the implications for NBZ phenomena, including solar wind capture, the low-latitude boundary layer and cold, dense plasma sheet

Dual-Lobe Reconnection and Horse-Collar Auroras

S. E. Milan[1,2] (ID), J. A. Carter[1] (ID), G. E. Bower[1], S. M. Imber[1] (ID), L. J. Paxton[3] (ID), B. J. Anderson[3] (ID), M. R. Hairston[4] (ID), and B. Hubert[5] (ID)

[1]School of Physics and Astronomy, University of Leicester, Leicester, UK, [2]Birkeland Centre for Space Sciences, University of Bergen, Bergen, Norway, [3]Johns Hopkins University Applied Physics Laboratory, Laurel, MD, USA, [4]William B. Hanson Center for Space Sciences, University of Texas at Dallas, Richardson, TX, USA, [5]Laboratory of Planetary and Atmospheric Physics, University of Liège, Liege, Belgium

Abstract We propose a mechanism for the formation of the horse-collar auroral configuration during periods of strongly northward interplanetary magnetic field (IMF), invoking the action of dual-lobe reconnection (DLR). Auroral observations are provided by the Imager for Magnetopause-to-Aurora Global Exploration (IMAGE) satellite and spacecraft of the Defense Meteorological Satellite Program (DMSP). We also use ionospheric flow measurements from DMSP and polar maps of field-aligned currents (FACs) derived from the Active Magnetosphere and Planetary Electrodynamics Response Experiment (AMPERE). Sunward convection is observed within the dark polar cap, with antisunward flows within the horse-collar auroral region, together with the NBZ FAC distribution expected to be associated with DLR. We suggest that newly closed flux is transported antisunward and to dawn and dusk within the reverse lobe cell convection pattern associated with DLR, causing the polar cap to acquire a teardrop shape and weak auroras to form at high latitudes. Horse-collar auroras are a common feature of the quiet magnetosphere, and this model provides a first understanding of their formation, resolving several outstanding questions regarding the nature of DLR and the magnetospheric structure and dynamics during northward IMF. The model can also provide insights into the trapping of solar wind plasma by the magnetosphere and the formation of a low-latitude boundary layer and cold, dense plasma sheet. We speculate that prolonged DLR could lead to a fully closed magnetosphere, with the formation of horse-collar auroras being an intermediate step.

Plain Language Summary During quiet geomagnetic conditions, the global distribution of auroras can acquire a "horse-collar" configuration, in which regions of weak auroral emission appear at dawn and dusk poleward of the main auroral oval. We propose a new model to explain the formation of this configuration, which provides new insights into magnetospheric dynamics during periods of northward-directed interplanetary magnetic field. To support our proposal, we use observations of the auroras, ionospheric convection, and estimations of the pattern of electrical currents flowing between the ionosphere and magnetosphere from a suite of spacecraft. Our proposed model resolves a 40-year-old question regarding the nature of the horse-collar auroras and many other aspects of magnetospheric dynamics.

1. Introduction

It has been known since space-based auroral imagery was first available that during prolonged periods of northward-directed interplanetary magnetic field (IMF) the auroral oval can resemble a "horse-collar" and the usually round polar cap becomes teardrop-shaped (e.g., Elphinstone et al., 1993; Hones et al., 1989; Murphree et al., 1982). Figure 1 compares the location of the main auroral oval for active geomagnetic conditions with that which can arise during persistent quiet times. During quiet times the oval contracts to higher latitudes and the dawn and dusk sectors contain weak (even subvisual) auroras poleward of the main oval. The location of the polar cap boundary, which delineates regions of open field lines at high latitudes and closed field lines, is shown in red. Although this is a common occurrence, to date the cause has not been satisfactorily elucidated. Previous studies have suggested that the horse-collar region maps to the magnetotail flanks and may be associated with the low-latitude boundary layer (Elphinstone et al., 1993), but without an understanding of how such a morphology arises; also, associated ionospheric flow patterns have been proposed, invoking lobe and viscous convection cells (Burch et al., 1992; Henderson et al., 1996), but
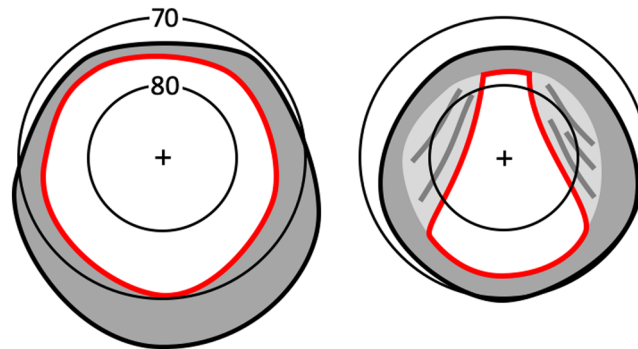
Figure 1. A schematic of the location of the main auroral oval during active conditions (left) and during quiet times (right) when a "horse-collar" auroral morphology can develop, with weak auroras seen at high latitudes in the dawn and dusk sectors and the polar cap (boundary shown in red) becomes teardrop-shaped. The regions of horse-collar auroras can exhibit multiple sun-aligned arcs. Noon is to the top, and circles represent lines of geomagnetic latitude.

these have failed to conform with subsequent observations. It is the aim of this paper to explain the formation of the horse-collar auroras (HCAs) within the context of the expanding/contracting polar cap (ECPC) model of magnetospheric dynamics (Cowley & Lockwood, 1992; Dungey, 1961), and by doing so provide a unifying picture of many northward IMF (NBZ) phenomena, including polar cap arcs, cusp auroras, and lobe reconnection.

Auroral features that appear when the north-south component of the IMF is positive ($B_Z > 0$) include polar cap arcs, transpolar arcs, sun-aligned arcs, or bending arcs (see reviews by Zhu et al., 1997, and Hosokawa et al., 2020), cusp spots (Carter et al., 2020; Frey et al., 2002; Milan et al., 2000), and high-latitude detached arcs or HiLDAs (Carter et al., 2018; Frey, 2007). Many of these phenomena are understood to be a consequence of magnetic reconnection (Dungey, 1961) occurring in the magnetotail or between the IMF and the high- or low-latitude dayside magnetopause. High-latitude reconnection typically occurs between the IMF and the magnetotail lobes, tailward of the cusps. This is referred to as dual-lobe reconnection (DLR) if the same IMF field line is reconnected with both northern and southern lobes, or single-lobe reconnection (SLR) if the process occurs independently in the two hemispheres (Cowley, 1981; Dungey, 1963). In this paper we argue that HCAs are a manifestation of DLR, with significant consequences for our understanding of the large-scale structure and dynamics of the magnetosphere during northward IMF. We also place the HCAs in the context of the ECPC model of magnetospheric convection (Cowley & Lockwood, 1992; Milan, 2015) and the other NBZ phenomena mentioned above.

Auroral features contained within the otherwise dark polar cap and approximately aligned parallel to the noon-midnight meridian are a common feature during NBZ conditions. Under the umbrella term "polar cap arcs" (PCAs) these have acquired various names with sometimes only a loose phenomenological (and, until recently, causal) distinction between them. The following taxonomy has slowly developed. "Sun-aligned arcs" (perhaps more accurately called "cusp-aligned arcs," Y. Zhang et al., 2016) are relatively dim auroral features which are thought to be produced by field-aligned currents (FACs) associated with shear flows in the polar cap convection pattern (Burke et al., 1982; Carlson & Cowley, 2005; Hardy et al., 1982; Q.-H. Zhang et al., 2020). Relatively bright "transpolar arcs" (TPAs) or "theta auroras" appear to grow from the nightside auroral oval to almost bisect the polar cap (Frank et al., 1982); after formation these arcs can progress dawnward and duskward across the polar cap in response to changes in the east-west (B_Y) component of the IMF. Such arcs have also been argued to be associated with ionospheric convection shears (see discussion in Cumnock & Blomberg, 2004). However, so far the most successful model explaining the formation of TPAs invokes reconnection in a twisted magnetotail producing a tongue of closed magnetic flux that protrudes into the polar cap and dayside reconnection for the subsequent motion of this flux (Fear et al., 2014; Fear & Milan, 2012a, 2012b; Goudarzi et al., 2008; Milan et al., 2005). The auroral emission of the TPA is produced by precipitation of plasma sheet-like particles trapped in this magnetic field configuration (Fear et al., 2014) which potentially reaches many tens of Earth radii (R_E) down-tail (Milan et al., 2020). A consequence of their closed nature is that TPAs are expected to occur simultaneously in both northern and southern hemispheres, though there is debate over whether this occurs (Carter et al., 2017; Craven et al., 1991;
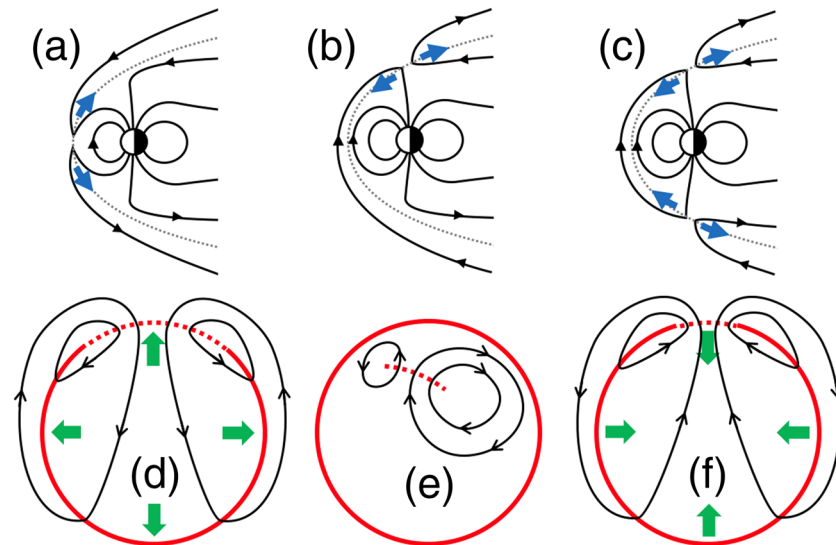
Figure 2. Schematic representations of the cross-section of the magnetosphere when (a) magnetic reconnection is active at the low-latitude magnetopause, (b) single-lobe reconnection (SLR) is ongoing in the northern hemisphere, and (c) dual-lobe reconnection (DLR) is occurring. Magnetic field lines are shown in black, the location of the magnetopause is the gray dotted line, and blue arrows indicate plasma flows away from the reconnection x-lines. (d) The expected ionospheric flow pattern for low-latitude reconnection, IMF $B_Z < 0$, $B_Y \approx 0$. Noon is to the top, and dawn to the right. The red circle indicates the open/closed field line boundary (OCB), with the ionospheric projection of the reconnection x-line shown dotted. Convection streamlines are presented in black. Green arrows indicate the motion of the OCB. (e) Expected flow pattern in the northern hemisphere for SLR, IMF $B_Z > 0$, $B_Y > 0$. (f) The ionospheric flow pattern proposed by Chisham et al. (2004) and Imber et al. (2006) for DLR, IMF $B_Z > 0$, $B_Y \approx 0$. It was assumed that the main auroral oval, at the equatorward edge of the OCB, would also progress poleward with time.

Østgaard et al., 2003). "Bending arcs" are auroral features that protrude into the polar cap from the dawnside or duskside auroral oval and progress over time toward the nightside, which are now thought to be created by low-latitude magnetopause reconnection, in a manner similar to poleward-moving auroral forms associated with flux transfer events, during B_Y-dominated IMF (Carter et al., 2015; Kullen et al., 2002, 2015). Finally, polar cap arcs have also been identified as the poleward edge of a thickened plasma sheet in the dawn and/or dusk sectors (Meng, 1981; Newell et al., 2009), that is, at the polar cap boundary of the HCAs, the subject of this paper. At times, polar cap arcs of different origins have been shown to coexist (Reidy et al., 2018, 2020).

When the IMF is directed southward, low-latitude magnetopause reconnection (Figure 2a) causes an increase in the open magnetic flux content of the magnetosphere, an enlargement of the polar caps, with antisunward flow within the polar caps and sunward return flow at lower latitudes, often described as the "twin-convection cells" of the Dungey cycle, as sketched in Figure 2d (Cowley & Lockwood, 1992; Dungey, 1961). Lobe reconnection is noted for producing sunward-directed ionospheric convection in the noon-sector polar cap, forming "lobe reverse convection cells" (e.g., Reiff, 1982). The exact form of these reverse cells depends on the B_Y component of the IMF, having a dawn-dusk asymmetry if $B_Y \neq 0$ (Reiff & Burch, 1985), shown in Figures 2b and 2e. In these cases, lobe field lines in one hemisphere are reconnected with the IMF to become disconnected from the magnetosphere at one end and draped over the nose of the magnetosphere at the other: SLR. Initially, the magnetic tension force on these draped field lines causes sunward convection. Then the combined action of the magnetosheath flow and B_Y-associated tension forces causes the field lines to be carried around the dawn and dusk flanks of the magnetosphere; whether more flux is carried dawnward or duskward, and hence whether the dawn or dusk lobe convection cell dominates, depends on the polarity of B_Y (e.g., Milan et al., 2005): Figure 2e shows the asymmetry expected in the northern hemisphere for $B_Y > 0$. Two auroral phenomena are associated with lobe reconnection: Direct precipitation of magnetosheath plasma along the newly reconnected field lines can produce a "cusp spot" downstream of the ionospheric projection of the reconnection site (Carter et al., 2020; Frey et al., 2002; Milan et al., 2000); upward FAC associated with the vorticity of the dawn lobe cell can produce "high-latitude detached arcs" or HiLDAs (Carter et al., 2018; Frey, 2007). Figure 2b shows SLR occurring in the northern

hemisphere: It can occur simultaneously in the southern hemisphere, though independently and possibly at a different rate.

If $B_Y \approx 0$ it is thought that the same IMF field line can reconnect with both northern and southern lobes (Figure 2c), eroding open lobe flux and creating newly closed magnetic field lines draped over the nose of the magnetosphere (Cowley, 1981; Dungey, 1963; Song & Russell, 1992). Chisham et al. (2004) and Imber et al. (2006) argued that this DLR should produce sunward ionospheric flow out of the noon-sector polar cap and a contraction of the polar cap as a whole, in both northern and southern hemispheres, as shown in Figure 2f. Imber et al. (2006, 2007) and Marcucci et al. (2008) did indeed find instances of this occurring and estimated from observational and theoretical considerations that DLR should occur for IMF clock angles $|\theta| < 10°$, where $\theta = atan2(B_Y, B_Z)$. The accumulation of closed field lines at the nose of the magnetosphere, possibly mass-loaded with captured solar wind plasma, has then been argued to progress tailward over time, maybe through a viscous interaction with the magnetosheath flow, and contribute to the formation of the northward IMF "low-latitude boundary layer" or LLBL (e.g., Sandholt et al., 1999; Song & Russell, 1992; Scholer & Treumann, 1997) and a "cold, dense plasma sheet" or CDPS in the magnetotail (e.g., Imber et al., 2006; Øieroset et al., 2005; Taylor et al., 2008; Terasawa et al., 1997; Wing et al., 2006). Although this aspect of the interaction has received significant attention, there are observational difficulties in its study (a notable exception being Fuselier et al., 2015). The problem has been further obfuscated by a poor understanding of the range of clock angles over which DLR occurs (Fuselier et al., 2014), the role of viscous processes in mass transport within the magnetosphere (Axford & Hines, 1961), and the possibility that the Kelvin-Helmholtz instability (KHI) is responsible for the formation of the CDPS by allowing direct entry of solar wind plasma into the flanks of the magnetosphere (Taylor et al., 2008).

We hope to resolve many of these controversies by arguing that the occurrence of DLR manifests itself in the ionosphere as the formation of HCAs, providing for the first time a satisfactory mechanism for their production which fits naturally into the scheme developed to explain other facets of magnetospheric dynamics. Our model helps clarify the structural changes that take place in the magnetosphere during periods of NBZ and facilitates quantification of the rates of DLR and of solar wind capture by the magnetosphere. The model we propose to replace the picture of Figure 2f is presented in Figures 3a–3c. In this model, the flux newly closed by DLR is not redistributed equally to all local times but is added progressively at dawn and dusk, eroding the polar cap to a teardrop shape. The regions of weak auroral emission and sun-aligned arcs forming the HCAs coincide with the location of newly closed flux. A key prediction of the model is that sunward ionospheric flows are contained within the remaining polar cap, and antisunward flows are located in the regions of HCAs. We present observations in support of this model in section 2. In section 3 we explain the model in more detail and discuss some of its ramifications. Finally, we conclude in section 4.

2. Observations

We show three intervals of data. In the first, we employ observations of the auroras and ionospheric flows from the Defense Meteorological Satellite Program (DMSP) F16 and F18 satellites. The DMSP satellites are in sun-synchronous orbits roughly aligned with the dawn-dusk meridian near an altitude of 850 km. The Ion Driftmeter (IDM) component of the Special Sensors-Ions, Electrons, and Scintillation thermal plasma analysis package or SSIES (Rich & Hairston, 1994) on F16 and F18 measured the cross-track horizontal ionospheric convection flow at 1-s cadence (approximately 7-km spatial resolution) along the orbit. The Special Sensor Ultraviolet Spectrographic Imager or SSUSI experiment (Paxton et al., 1992) recorded a swath of auroral luminosity, extending sunward and antisunward from the orbit, in five wavelength bands. We use observations at 130.4 nm, which measures emissions associated with electron precipitation-induced O I auroral transitions, and the Lyman-Birge-Hopfield short (LBHs) band, 140 to 152 nm, sensitive to emissions produced by soft electron precipitation. Each pass of the polar regions by a DMSP spacecraft takes 15 to 20 min. We combine these with measurements of the magnetosphere-ionosphere coupling FACs from the Active Magnetosphere and Planetary Electrodynamics Response Experiment (AMPERE), derived from magnetometer measurements onboard the satellites of the Iridium telecommunications constellation (Anderson et al., 2000; Coxon et al., 2018; Waters et al., 2001). FACs are derived on a grid of 24 magnetic local time (MLT) sectors divided into fifty 1° bins of geomagnetic latitude, at a cadence of 2 min. We average the FACs over the duration of each DMSP pass.
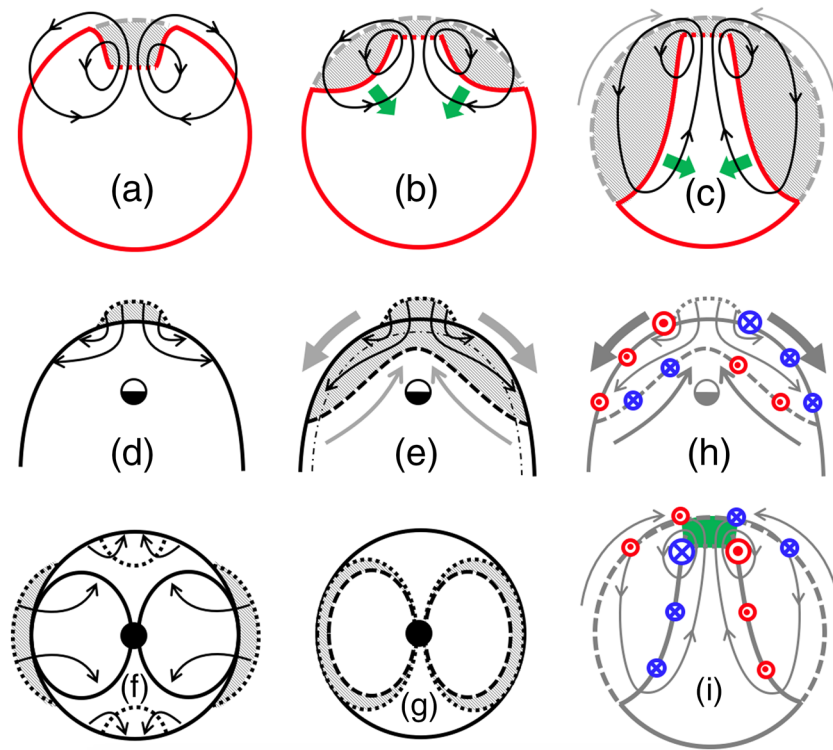
Figure 3. (a–c) Our proposed model for the formation of horse-collar auroras by dual-lobe reconnection, in a similar format to Figures 2d–2f. The shaded region indicates newly closed flux produced by DLR, which is redistributed to dawn and dusk. As time progresses, the OCB moves poleward at dawn and dusk to assume a teardrop shape. The main auroral oval remains relatively unchanged, located equatorward of the circular outline. Flows associated with a viscous solar wind interaction, if it occurs, are indicated by gray arrows. (d) The equatorial plane ($Z = 0$) of the magnetosphere. A region of newly closed flux is appended to the nose of the magnetosphere by DLR; flows are excited within the magnetosphere (arrows) to return the magnetopause to stress balance with the flow of the solar wind. (e) As more closed flux is appended, magnetic flux laden with captured solar wind plasma moves to dawn and dusk, forming a boundary layer inside the magnetopause (the width of this boundary layer is exaggerated for clarity); the original position of the magnetopause is shown as a dot-dashed line. Flows associated with a viscous solar wind interaction are shown in gray. (f) The cross-section of the magnetosphere ($X = 0$). The dipolar lines show the separatrix between closed and open flux regions, with open lobe flux at the top and bottom. DLR removes open flux from the north and south (dotted regions) and appends newly closed flux first at noon and then at the dawn and dusk flanks. Flows are excited to return the magnetosphere to a circular cross-section. (g) The location of the newly closed, solar wind plasma laden field lines once equilibrium is re-attained. This flux maps to the dawn and dusk horse-collar auroras in the ionosphere. (h and i) Expected field-aligned current (FAC) regions associated with the magnetospheric dynamics driven by dual-lobe reconnection in the equatorial plane of the magnetosphere and the ionosphere. These include the NBZ FACs in the dawn and dusk portions of the dayside polar cap. The expected location of cusp spot auroras produced by magnetosheath precipitation downstream of the ionospheric projection of the reconnection site is indicated in green.

The lower panel of Figure 4 shows the IMF conditions for the interval, accessed from the National Aeronautics and Space Administration OMNIWeb portal (King & Papitashvili, 2005). The upper panels present a series of passes of the DMSP satellites over the northern and southern hemispheres (NH and SH) on 15 December 2015. The two left-hand columns show the FACs measured by AMPERE in the two hemispheres. The IMF $B_Y - B_Z$ component vector is shown between these panels. Depending on whether the spacecraft pass is over the NH or SH, the orbital track is indicated in one or other of these panels, with the IDM cross-track plasma flow measurements superimposed. To the right are the corresponding auroral observations in the two wavelength bands.

During the interval of interest, 14:43 to 20:40 UT, the magnitude of the IMF varied in the range 7 to 10 nT, and its orientation rotated from southward but B_Y-dominated, to almost purely northward, and back to B_Y-dominated. At the start of the interval, 14:43 UT, the IMF had components $B_Y \approx -5$ and $B_Z \approx -2$ nT. The FAC patterns were dominated by the expected Region 1 and 2 (R1 and R2) current systems (Iijima & Potemra, 1976), and the ionospheric flows were consistent with twin-cell convection with an east-west

Figure 4. Observations from AMPERE and DMSP F16 and F18 during 15 December 2015, an interval when horse-collar auroras developed, associated with a northward turning of the IMF. Six rows show different passes of the two DMSP spacecraft. On the left is presented the field-aligned currents observed by AMPERE in the northern and southern hemispheres (we suppress $|j_{||}| < 0.1\,\mu\mathrm{A\,m^{-2}}$ to remove noise). Concurrent IMF B_Y and B_Z components are shown in the inset panel, in which the radius of the circle represents 10 nT. The satellite track and cross-track ionospheric flow measured by DMSP/SSIES is displayed over the hemisphere in which the pass occurred. On the right, the corresponding auroras observed by DMSP/SSUSI are displayed. Observations are shown in a geomagnetic latitude and magnetic local time format, with noon to the top and dawn and dusk to the left and right; colatitudes in steps of 10° are represented by circles. The lower panel shows the IMF B_Y (green) and B_Z (red) components for the interval, together with the total field strength $\pm B_T$ (gray). The clock angle (blue) is superimposed.

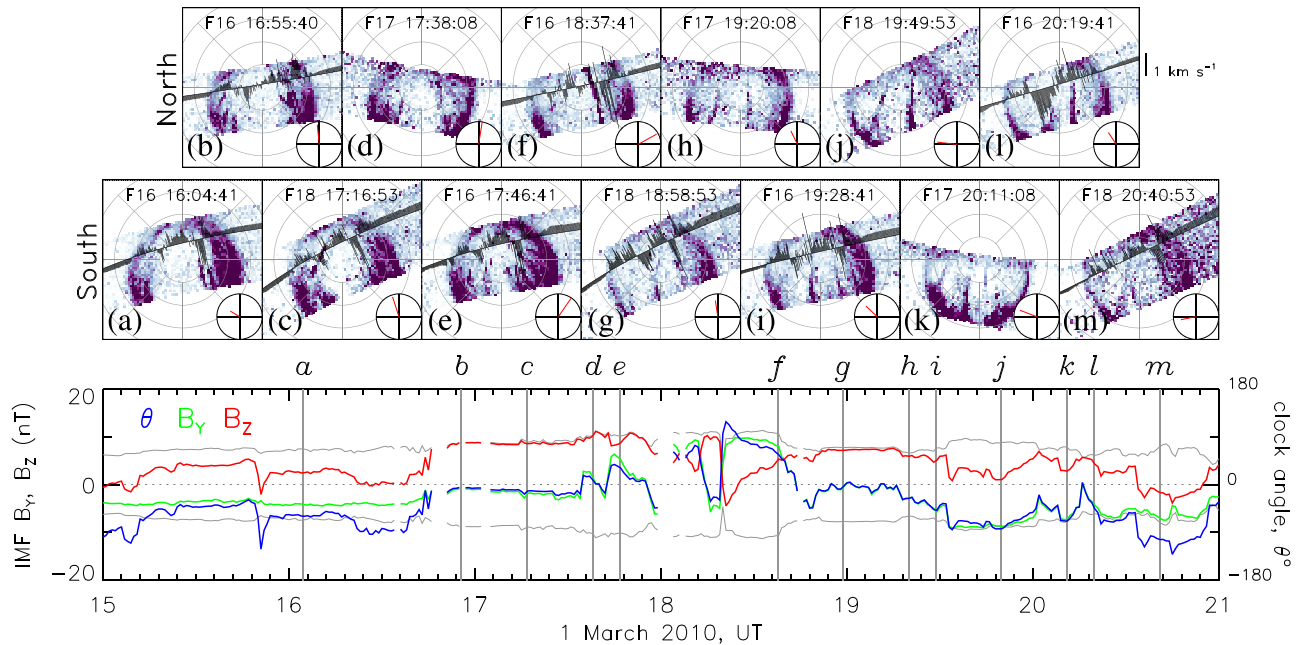**Figure 5.** (a–m) DMSP/SSIES and DMSP/SSUSI (LBHs emissions) observed by DMSP F16, F17, and F18 on 1 March 2010, presented in a similar format to Figure 4; passes of the northern and southern hemisphere are shown above and below. (bottom) The IMF B_Y (green) and B_Z (red) components, together with the total field strength, $\pm B_T$ (gray). The clock angle (blue) is superimposed.

asymmetry consistent with $B_Y < 0$. The corresponding auroral configuration showed a main auroral oval that was located equatorward of 70° latitude, with an expanded polar cap. The polar cap continued to expand after this time, until a substorm onset occurred around 15:30 UT (not shown). By 16:25 UT, the IMF had components $B_Y \approx -4$ and $B_Z \approx +3$ nT, the polar cap was somewhat contracted from previously (due to the substorm), and the FACs and ionospheric flows were consistent with lobe-stirring (we note that the R1/R2 FACs are strongest at dusk and dawn in the NH and SH, respectively, where the flow shear between open and closed field lines is strongest), which we expect to be driven by SLR.

At 17:29 and 18:20 UT, the IMF rotated to being northward, $B_Y \approx -1$ and $B_Z \approx +7$ nT, before beginning to become B_Y-dominated again, $B_Y \approx -5$ and $B_Z \approx +2$ nT, at 19:11 UT. Especially at 18:20 and 19:11 UT, the FACs had the characteristic NBZ pattern associated with symmetrical lobe reverse cells, though stronger in the SH than the NH due to solar illumination in the summer hemisphere and enhanced conductance. The ionospheric flows showed sunward motions in the central polar cap and antisunward motions in the dawn and dusk sectors, again consistent with lobe reverse cells. (We note that Reidy et al., 2020, have presented Super Dual Auroral Radar Network [SuperDARN] convection measurements, Chisham et al., 2007, from this interval, see their Figure 10, which corroborate this flow pattern.) Over this period, sun-aligned auroral features appeared poleward of the dawn and dusk sector main oval: the horse-collar auroral configuration that is the subject of this paper. The polar cap became teardrop-shaped and progressively smaller with time as the auroras moved to higher latitudes. At 19:11 UT there was a prominent sun-aligned arc at the poleward edge of the dawn HCA, colocated along much of its length with an upward FAC (indicated by an arrow); a similar downward FAC (second arrow) was colocated with the poleward edge of the dusk HCA and a fainter sun-aligned arc. A key observation is that the sunward ionospheric flows were located within the dark polar cap, whereas the antisunward flows were within the dawn and dusk regions of the developing HCA (cf. Figure 3c). We will argue below that DLR was occurring during this period, and the HCAs are the result of open magnetic flux being closed and redistributed to the dawn and dusk sectors.

By 20:40 UT, the IMF was B_Y-dominated again, asymmetrical twin-cell convection was ongoing, and the opening of magnetic flux by low-latitude reconnection had caused the polar cap to re-expand once again.

Next, in Figure 5 we present the interval 15 to 21 UT on 1 March 2010. The bottom panel shows the IMF B_Y and B_Z components, as well as the IMF clock angle, for the interval. Top panels show passes of the northern and southern hemispheres by DMSP F16, F17, and F18. Emissions in the LBHs band detected by SSUSI

are presented (note that the color scale has been adjusted in individual panels to emphasize weak auroral features), with IDM cross-track drift vectors superimposed when measurements are reliable. (The IDM data quality can become poor if the ratio of H^+ and He^+ to O^+ exceeds 20%, which occurs most frequently at solar minimum and in the winter hemisphere). At the start of the interval (panel a), $B_Z \approx +5$, $B_Y \approx -5$ nT, the polar cap was empty, and the ionospheric flows were consistent with SLR (see Figure 2e). Over panels (b) and (c) the IMF turned northward, $B_Z \approx +10$ nT, clock angle $|\theta| < 10°$, and the flows evolved to be sunward in the central polar cap and antisunward at dawn and dusk. HCAs developed, seen most clearly in panel (d), and moved progressively poleward, as seen in panel (e). Over the next hour both B_Y and B_Z components changed rapidly, and the flows in the ionosphere became more complicated (panel f); indeed, it is likely that the flow pattern was changing as the spacecraft traversed the polar regions. The IMF clock angle became close to 0° again during panels (g) and (h), and the HCAs were still discernible, but they were now displaced, toward dawn in the SH and dusk in the NH. Subsequently, the IMF turned to be B_Y-dominated, with $B_Y < 0$, the flow patterns became consistent with lobe-stirring, anticlockwise in the NH (panel l) and clockwise in the SH (panel m), and the arcs moved toward dawn and dusk, respectively. It is possible that the arcs are displaced dawn-dusk to different degrees in the two hemispheres.

We inspected AMPERE and DMSP data for the period 2010 to 2016 (the period that AMPERE data are currently available) for other instances of the formation of HCAs. Similar sequences of events—purely northward IMF, symmetric NBZ FACs, and the development of HCA with sunward flow in the polar cap and antisunward flow within the HCA—are a common and reproducible feature of the data (indeed, similar observations have been widely reported in the literature; see, e.g., Figure 8 of Cumnock & Blomberg, 2004, as well as Figure 10 of Reidy et al., 2020). We will present a statistical survey of the events in a subsequent paper.

Now, we discuss an interval observed from the Imager for Magnetopause-to-Aurora Global Exploration (IMAGE) spacecraft with the FUV instrument (Mende, Heetderks, Frey, Lampton, Geller, Abiad, et al., 2000; Mende, Heetderks, Frey, Lampton, Geller, Habraken, et al., 2000; Mende, Heetderks, Frey, Stock, et al., 2000), comprising the Wide-band Imaging Camera (WIC), which mainly measured LBH auroral emissions between 140 and 190 nm produced by precipitating electrons, and the Spectrographic Imager (SI12), which observed Ly-α proton auroras. HCAs have not been widely reported in IMAGE observations, and we suspect that the cameras are relatively insensitive to these weak auroral features. The interval of interest is 24 November 2001 during which IMAGE was observing the northern hemisphere, as presented in Figure 6. This is an extreme interval, during which the solar wind speed approached 1,000 km s^{-1}, the density was variable about an average of 25 cm^{-3}, and the IMF magnitude was near 70 nT. We think that under these conditions DLR created HCAs that were at the limit of detection by IMAGE.

Panels (a) and (b) show the WIC and SI12 observations averaged between 10:20 and 10:30 UT. A prominent cusp spot was observed at this time, a period of strongly northward IMF ($B_Y \approx +14$, $B_Z \approx +51$ nT). DMSP F13 passed across this cusp feature, recording sunward flows of 2 km s^{-1} colocated with the spot (corresponding to a voltage of approximately 80 kV) and antisunward flows of 1 km s^{-1} either side (IDM on DMSP F13 had a temporal cadence of 4 s corresponding to a measurement every 28 km). Although we might expect HCAs to be forming or have formed at this time (as per the previous examples), there is little evidence for them. However, a weak (in comparison to the brighter main oval) auroral arc was associated with the dawnside edge of the cusp spot in the WIC image (indicated by an arrow), and weak auroral emission in the high-latitude dawn sector was observed by both cameras. An hour later (panels c and d), the IMF had rotated to be southward but B_Y-dominated ($B_Y \approx -40$, $B_Z \approx -23$ nT). DMSP F13 crossed the SH and observed flows consistent with a standard twin-cell convection pattern with the expected dawn-dusk asymmetry (we have mirrored the DMSP track across the noon-midnight meridian to represent the flows as we expect they would appear in the NH). There was no longer a cusp spot, the main auroral oval had moved to low latitudes, and the polar cap had expanded, an indication that low-latitude magnetopause reconnection had created new open magnetic flux. As this auroral configuration developed, the dawn and dusk sector weak auroras we expected to see in panels (a) and (b) brightened and became more evident (indicated by arrows). These became deformed by the redistribution of magnetic flux in the polar regions represented by the ionospheric flow pattern, being transported antisunward and dawnward, with new open flux occupying the dayside polar cap.
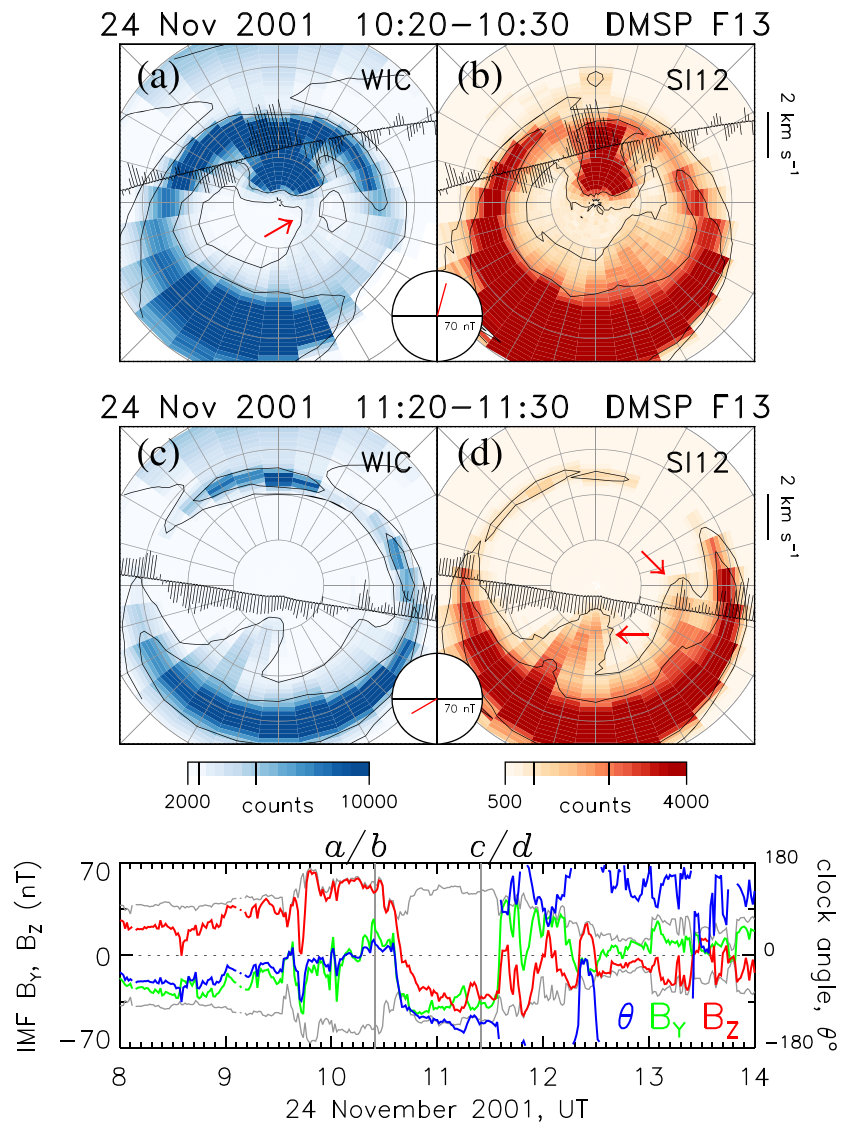
Figure 6. Images of the northern hemisphere auroras observed by WIC and SI12 onboard IMAGE during two periods, 10:20 to 10:30 and 11:20 to 11:30, on 24 November 2001. Two contours are added on the emissions to guide the eye. The inset panel shows the B_Y and B_Z components of the IMF, in which the radius of the circle represents 70 nT. Superimposed is the satellite track and cross-track ionospheric flow measured by DMSP/SSIES onboard DMSP F13. In the top panels, F13 overpasses the northern hemisphere; in the bottom panels the pass is in the southern hemisphere, and the track and flow measurements have been mirrored about the noon-midnight meridian, to reflect the sense of the convection expected in the northern hemisphere. The lower panel shows the IMF B_Y (green) and B_Z (red) components for the interval; the total magnetic field strength, B_T, is shown in gray. The clock angle (blue) is superimposed.

3. Discussion

During southward IMF ($B_Z < 0$), dayside reconnection creates open magnetic flux which forms the magnetotail lobes; subsequently, nightside reconnection closes flux which returns to the dayside, leading to the Dungey cycle of convection (Dungey, 1961). As described by the ECPC model of magnetospheric and ionospheric convection (Cowley & Lockwood, 1992; Milan, 2015), the amount of open magnetic flux in the magnetosphere, which dictates the size of the polar cap, is a competition between the rates of dayside and nightside reconnection (Milan et al., 2007); at all times the polar cap remains approximately circular due to the pressure of the solar wind on the magnetopause, the main motivating force for the redistribution of magnetic flux within the magnetosphere. Figure 2d shows the expected ionospheric flow pattern and expansion of the polar cap for dayside but no nightside reconnection.

When $B_Z > 0$ and $B_Y \neq 0$, SLR merges the IMF with open magnetic flux of the lobes to create new open lobe field lines, the open flux content remains unchanged, and the flux within the polar cap is stirred, as shown in Figure 2e, forming a major "reverse convection cell" with possibly a second, minor cell. The polar cap tends to remain circular, but processes can give rise to auroral features poleward of the main oval, sometimes associated with open field lines, and sometimes closed (see discussion in section 1).

In this paper, we specifically discuss the behavior when $B_Z > 0$ and $B_Y \approx 0$, clock angles $\theta \approx 0°$, when DLR is expected to occur. Now open field lines of the lobes are closed and result in new closed flux draped over the dayside magnetopause. Chisham et al. (2004) and Imber et al. (2006) reasoned that this should result in convection flows sunward across the dayside open/closed field line boundary or OCB (synonymous with the polar cap boundary) and a general contraction of the polar cap to higher latitudes; the scenario they suggested is shown in Figure 2f, essentially the reverse of the situation suggested by Cowley and Lockwood (1992) for southward IMF (Figure 2d). Imber et al. (2006, 2007) and Marcucci et al. (2008) did indeed find instances of the expected flows, but significant contraction of the polar cap was not evident. In this study, we argue that the true signature of polar cap contraction was missed by previous workers because the OCB does not move poleward equally at all local times, but does so predominantly at dawn and dusk to create the teardrop shape associated with HCAs. We suggest that this occurs progressively, as indicated in Figures 3a–3c.

Figure 3a shows that a region of dayside open flux has been closed by DLR, exciting sunward convection flows across the reconnecting portion of the OCB (dotted), which turn dawnward and duskward due to the magnetic tension force and the flow of the magnetosheath. The ionospheric convection pattern requires interchange flows to close the streamlines, leading to polar cap motions excited by stresses imposed on the magnetopause by the pressure of the solar wind (see below). Where the streamlines cross "adiaroic" portions of the OCB (away from the reconnecting portion of the boundary, Siscoe & Huang, 1985), the flows and boundary move together, carrying the OCB poleward (Figure 3b, green arrows), beginning to form a teardrop-shaped polar cap. As open flux continues to be closed, the poleward motion of the OCB progresses around the flanks of the polar cap (Figure 3c). The newly closed magnetic flux now occupies the high-latitude dawn and dusk sectors, and particle precipitation on these field lines creates the horse-collar auroral configuration. As DLR continues, the polar cap will continue to shrink, with the HCAs expanding to ever-higher latitudes. Non-zero B_Y could lead to differences in the convection in the dawn and dusk reverse cells and hence asymmetries in the size of the dawn and dusk HCA regions, subject to the constraint that the amount of newly closed flux at dawn is equal in both northern and southern hemispheres, with the same applying to dusk.

The associated flows in the equatorial plane of the magnetosphere ($Z = 0$) are illustrated in Figures 3d and 3e, whereas Figures 3f and 3g show the $X = 0$ plane. Figure 3d corresponds to the situation in Figure 3a: A pulse of DLR has created a region of closed magnetic flux draped across the dayside magnetosphere (dotted outline and shaded region). The magnetopause is no longer in magnetohydrodynamic stress balance with the flow of the solar wind, and motions are excited within the magnetosphere to return it to a stream-lined bullet shape. As DLR continues, Figure 3e, the dayside region of the magnetosphere becomes increasingly occupied by newly closed flux, and this will begin to be pushed antisunward around the flanks (the demarcation between old and new closed flux is indicated by a dashed line; the width of the new boundary region, shown shaded, is exaggerated for clarity). This antisunward progression may be aided by viscous processes associated with the flow of the solar wind (thick gray arrows); in this case, return flows will be required in the inner magnetosphere (thin gray arrows). As the open flux content of the magnetosphere decreases, the cross-sectional area of the closed flux in the equatorial plane will increase and the magnetopause will move outward (the original position of the magnetopause is shown by the dot-dashed line in Figure 3e).

The full lines in Figure 3f show the magnetospheric configuration before DLR, with a circular cross-section and an approximately dipolar field-shaped boundary separating the open lobes and closed field line regions. After DLR, the lobes are eroded at the top and the bottom, and new regions of closed field lines are appended first at noon, before being carried to the dawn and dusk flanks (dotted lines and shading). Flows are excited to return the magnetopause to an approximately circular cross-section; these flows mapping to the ionosphere to produce the patterns are indicated in Figures 3a–3c. Figure 3g shows the resulting cross-section, in which the lobes have shrunk, the dotted line indicating the new separatrix between open and closed field lines, and

the dashed line indicating the demarcation between old and new closed flux. The newly closed flux between the dotted and dashed lines maps to the location of the HCAs.

FACs are required to couple the magnetospheric and ionospheric phenomena described above, illustrated in the equatorial plane of the magnetosphere (Figure 3h) and in the ionosphere (Figure 3i). Blue and red circles indicate FACs into and out of the page, respectively. The vorticity of the reverse lobe convection cells requires a pair of upward and downward FACs, the familiar NBZ current system; this current system will be extended along the convection reversal boundaries at the poleward edges of the horse-collar auroral regions. All these FACs map to the magnetopause and can close across the nose of the magnetosphere through a dawn-to-dusk current, in a similar manner to the usual Chapman-Ferraro current. FACs will also be generated due to pressure gradients in the inner magnetosphere near the boundary between new and old closed flux (in a similar manner to usual Region 2 FACs) and will close through a dayside partial ring current. These FACs will map equatorward of the NBZ currents in the ionosphere, corresponding to the convection shear at the equatorward edge of the lobe cells (and any viscous flows, should they be present). Auroras might be expected to be produced in the ionosphere at the foot of upward FACs, produced by precipitating electrons. Auroras are known to be colocated with the upward NBZ FAC, known as high-latitude detached auroras or HiLDAs (Carter et al., 2018; Frey, 2007). Figure 3i also shows where auroras can form (green) due to direct precipitation of magnetosheath plasma downstream (sunward) of the footprint of the lobe reconnection site, to form an auroral cusp spot (Carter et al., 2020; Frey et al., 2002; Milan et al., 2000), which would be accompanied by a reverse ion dispersion signature (Woch & Lundin, 1992). The FAC pattern also indicates that auroras might be expected along the poleward edge of the dawn horse-collar region.

Now we compare the model predictions with the observations. The ionospheric flow pattern presented in Figure 3c, with sunward convection in the polar cap and antisunward convection in the region of weak HCAs, agrees with the observations in Figures 4 and 5. Symmetric NBZ FACs seen by AMPERE, and the SuperDARN flows reported by Reidy et al. (2020), corroborate that reverse lobe cells are present at the sunward portion of the HCAs. The FAC patterns predicted, including NBZ currents and FACs along the poleward edge of the HCAs, are present in Figure 4. The model also predicts the progressive evolution of the polar cap from circular to teardrop-shaped, which is a well-known feature of periods of HCAs. The location of the cusp spot predicted in Figure 3i agrees with Figures 6a and 6b.

Based upon magnetic modeling, Elphinstone et al. (1993) suggested that the HCA regions map to the magnetopause flanks and may be associated with the low-latitude boundary layer. Our model now explains how this magnetospheric morphology arises. Burch et al. (1992) and Henderson et al. (1996) proposed convection patterns that might be associated with HCA and TPAs: These invoked merging, lobe, and viscous cells. These flow patterns were static and did not explain how the magnetosphere evolved to the HCA/TPA configuration; they also predicted antisunward flow along the noon-midnight meridian, which is contrary to observations. These models correctly anticipated that magnetic reconnection is the architect of these NBZ morphologies but failed to consider the central role that DLR plays.

Flow shears have long been implicated in the formation of PCAs (e.g., Cumnock & Blomberg, 2004). However, when it was assumed that these flow shears occurred within the open polar cap, it was unclear why the shears should be sharp enough to produce thin auroral arcs, and be as long-lived as observations suggested. The model presented here places these flow shears at the boundary between open and closed field lines, hence necessarily producing the required spatial and temporal behavior. Although we should be careful not to over-interpret the observations, we note elongated, sun-aligned upward and downward FAC regions in Figure 4e, indicated by arrows, that are close to the flow reversals in the driftmeter data, as predicted in Figure 3i, and that are colocated with the brightest emissions at the poleward edges of the dawn and dusk HCAs. A similar, albeit faint, dawn arc is also seen in Figure 6a. Hence, the model also explains why polar cap arcs often form adjacent to regions of particle precipitation characteristic of trapped plasma on closed magnetic field lines, in other words, a thickened plasma sheet at dawn and dusk (e.g., Cumnock et al., 2002; Meng, 1981; Newell et al., 2009).

DLR has been postulated to be an efficient mechanism by which the magnetosphere can capture cold dense solar wind plasma (e.g., Imber et al., 2006; Sandholt et al., 1999; Song & Russell, 1992). The horse-collar region will then be associated with trapped dense plasma, which may give rise to weak or subvisual auroral emission. Time variability in the rate of DLR could structure this plasma, giving rise to features within these auroras, a possible explanation for the cusp-aligned arcs often seen within the HCAs. This trapped plasma
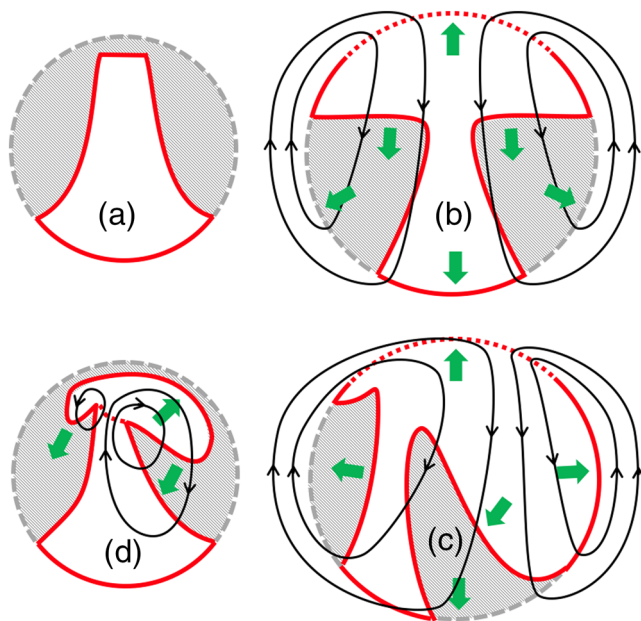
Figure 7. Anticipated response to a change in IMF orientation of (a) the original polar cap and horse-collar configuration. (b) A southward turning leads to the addition of new open flux to the dayside polar cap by low-latitude magnetopause reconnection, causing an expansion of the main auroral oval and a general antisunward motion of the horse-collar regions within the twin-cell convection pattern. (c) A similar situation but with $B_Y > 0$ (shown for NH) leads to the asymmetrical addition of new open flux and a general duskward motion of the closed flux at high latitudes. (d) Continued northward IMF but with $B_Y > 0$ drives single-lobe reconnection which siphons open flux from the preexisting polar cap and expands a new polar cap at dawn (and maybe a smaller one at dusk), causing closed flux to move together and duskward (in the NH).

could be related to observations of a low-latitude boundary layer adjacent to the flank magnetopause during periods of northward IMF (Scholer & Treumann, 1997; Song & Russell, 1992). Our model is consistent with the study by Lu et al. (2011), in which they reported an interval of northward IMF with reverse convection, NBZ FACs, and regions of precipitation at high latitudes, which they termed "NBZ boundary layer" (NBZBL), which we identify as our association between HCAs and an LLBL. In addition, Lu et al. (2011) presented the results of a simulation in which DLR was shown to be responsible for the formation of this configuration.

The internal boundary between the preexisting magnetosphere (containing hot and tenuous plasma) and the LLBL (containing cold, dense plasma) could be prone to an interchange instability or the KHI, which could corrugate the boundary and give rise to structured auroral emission within the horse-collar region (as shown in Figure 1). The KHI can also operate on the magnetopause, and it was recently suggested by Q.-H. Zhang et al. (2020) that this can give rise to flow shears that propagate into the magnetosphere and produce multiple polar cap arcs; the present model elucidates why closed magnetic flux is to be found at high latitudes, within which such arcs can form.

It has been further suggested that this captured solar wind plasma can contribute to the formation of a cold, dense plasma sheet or CDPS (Imber et al., 2006; Øieroset et al., 2005; Terasawa et al., 1997; Wing et al., 2006), though tracking the redistribution of this plasma in the magnetosphere was thought difficult (Fuselier et al., 2015). Here we argue that the HCAs represent the regions of trapped solar wind plasma, forming a low-latitude boundary layer inside the magnetopause, and by charting their development, this redistribution can be tracked. Once the plasma has been transported to the tail, mixing with the preexisting plasma sheet is thought to occur, though the mechanism by which this is achieved is unclear. Potentially, the KHI and interchange processes taking place at the boundary between the new and old closed flux contribute to this mixing and could be revealed by small-scale auroral or convection features in the ionosphere.

Convection measurements in the nightside polar regions during northward IMF regularly reveal disordered flows with multiple sunward/antisunward flows shears; as discussed above, these flow shears could be associated with the formation of sun-aligned arcs in both the open and closed field line regions. These disordered motions could be a signature of the mixing processes described previously, superimposed on the large-scale flows shown in Figure 3c. These observations also suggest that the excitation of convection associated with DLR, especially on the nightside, is a haphazard affair. The main driver of convection is the pressure of the solar wind exerted on the magnetosphere and the redistribution of magnetic flux within to achieve stress balance at the magnetopause (Cowley & Lockwood, 1992). DLR is associated with the removal of flux from the magnetotail lobes (Figure 3f), and this may manifest itself as sporadic and spatially incoherent polar cap flows.

In Figures 7b and 7c we illustrate how we expect the auroral morphology to evolve after a southward turning of the IMF. Panel (a) shows the preexisting horse-collar configuration. The onset of low-latitude magnetopause reconnection will lead to the creation of new open flux which will be appended to the dayside polar cap, abutting the dayside portion of the HCA (Figure 7b). As this region expands, there will be a general expansion of the main oval to lower latitudes and a redistribution of open and closed flux at higher latitudes, in the form of a twin-cell convection pattern, that pushes the HCA regions toward the nightside (cf. Figure 8c of Milan et al., 2005). If the convection pattern has a dawn-dusk asymmetry associated with a non-zero IMF B_Y (Figure 7c), then the regions will be deformed as seen in Figures 6c and 6d (cf. Goudarzi et al., 2008; Newell & Meng, 1995). Figure 7d sketches the evolution expected if the IMF remains northward but develops a non-zero B_Y (specifically shown in the NH for $B_Y > 0$): Now the open flux content of the

magnetosphere remains unchanged, but SLR siphons open flux from the preexisting polar cap and produces a new region of open flux at dawn (Milan et al., 2005); it is also possible that if a second, smaller reverse cell is present (Figure 2e), then a smaller open region at dusk could also form. SLR can occur at different rates in the two hemispheres, so arc motions in the NH and SH driven by this process can be independent of each other (see Figure 5). Considerations such as these can be used to explain many of the auroral configurations and evolutions reported in the literature, for instance, in the examples reported in Cumnock and Blomberg (2004). It is also possible that the dynamics sketched in Figure 7 could contribute to the formation of bending arcs (e.g., Kullen et al., 2015).

As we have shown, the HCAs are likely associated with a sun-aligned arc at the poleward boundary of the dawn sector closed flux. The regions of HCAs tend also to be filled with multiple sun-aligned arcs (see Figure 1). Mechanisms have been proposed that lead to (sometimes multiple) small-scale flow shears in both open and closed field line regions, which could drive FACs and hence produce auroras (e.g., Q.-H. Zhang et al., 2020). It is anticipated that the response of the polar regions to changes in the IMF, sketched in Figure 7, can explain the motions of such arcs. The mechanism proposed by Milan et al. (2005) to produce TPAs via nightside reconnection can also operate, though this will be confined to the open polar cap region. This mechanism would likely form TPAs adjacent to the HCAs if they have developed previously, and this could influence the range of local times at which TPAs are initially seen. The subsequent motion of a TPA is associated with changes in polarity of the B_Y component of the IMF (Milan et al., 2005; Valladares et al., 1994), suggesting conditions that are not favorable for DLR and the formation of HCAs, so again Figure 7 encompasses many of the possible configurations that can arise. As the IMF tends to undergo changes in orientation on timescales of minutes and hours and the lobe reconnection sites will move around, at some times undergoing DLR and at others SLR, we can expect a very complicated distribution of open and closed magnetic flux to develop in the polar regions. This could take the form of a complex interleaving of regions of open and closed magnetic flux and/or flow shears in the dawn and dusk regions, perhaps resembling the spatial distribution of multiple sun-aligned arcs. (This could also explain the mixture of open and closed particle populations in the NBZ low-latitude boundary layer.) As asserted by Fear et al. (2015), an understanding of how lobe reconnection interacts with both open and closed flux on the magnetopause is important for understanding all the magnetic geometries and structures that can arise.

A key prediction of the model proposed, for the formation of the HCS by DLR and the subsequent motions of features by SLR or low-latitude reconnection, is that the timescales involved are dependent on the reconnection rates. If an arc system is created solely by a convection reversal boundary, then in principle, in response to a change in the B_Y component of the IMF, that convection reversal can fade away and a new shear flow can form somewhere else in the polar cap almost instantaneously, in which case arcs could jump from one location to another. Observationally, PCA systems tend to move as a coherent feature, suggesting that they are associated with a long-lived magnetic structure (such as a region of closed flux). A quiet-time polar cap tends to contain less than 0.5 GWb of open flux (e.g., Milan et al., 2005, 2007). To close half of that, say 0.2 GWb, by DLR to form HCAs at a reconnection rate of 80 kV (Figure 6), would take 40 min. A lobe reconnection rate of 80 kV seems atypically high (and does occur during an interval of $B_Z \approx +50$ nT), but it is not unprecedented (Clauer et al., 2016). However, timescales of 1 to 2 hr might be more usual. Equally, the timescale for a TPA to move from one side of the polar cap to the other through lobe-stirring associated with SLR should be of the order of an hour or more, consistent with observations (e.g., Milan et al., 2005).

Finally, we speculate that if DLR precedes for long enough, the magnetosphere could close entirely. Y. Zhang et al. (2009) presented auroral observations from a period of strongly northward IMF which showed the polar regions filled with multiple discrete arcs. They suggested that DLR closed the polar cap completely but did so by eroding the dayside OCB from noon across to midnight. We believe that the formation of HCAs and the intrusion of the OCB at dawn and dusk by DLR, as an intermediate stage before full closure of the magnetosphere, is a more common scenario.

4. Conclusions

We have described how DLR occurring during periods of strongly northward IMF ($B_Z > 0$, $B_Y \approx 0$) can give rise to the formation of the common horse-collar auroral configuration, in which the polar cap becomes teardrop-shaped and weak auroras move to high latitudes in the dawn and dusk sectors. This naturally

explains many of the features of the northward IMF magnetosphere, including the capture of solar wind plasma by the magnetosphere and the formation of a low-latitude boundary layer and a cold, dense plasma sheet. This model provides a new understanding of the structure and dynamics of the magnetosphere, resolving many long-standing questions. We further suggest that if DLR continues for a prolonged period, then the magnetosphere can become entirely closed.

Once the HCA has formed, changes in the orientation of the IMF can lead to a number of different evolutions of the system, depending on whether high- or low-latitude magnetopause reconnection takes place and the B_Y component of the IMF. The creation of new open flux, or the redistribution of existing open flux, can lead to antisunward and/or east-west motions of auroral features, as open and closed flux regions alike are stirred within the polar regions. With changeable IMF, a complicated magnetic structure can arise.

Our model is an extension of the ECPC model first proposed in full by Cowley and Lockwood (1992), originally developed to explain the dynamics of the magnetosphere in response to low-latitude magnetopause reconnection (occurring for $B_Z < 0$) and substorm-related tail reconnection. This model was augmented by Milan et al. (2005) to show how magnetotail reconnection within a twisted tail ($B_Z > 0$, $B_Y \neq 0$) could give rise to tongues of closed magnetic flux intruding into the polar cap from the nightside to form transpolar arcs. Carter et al. (2015) explained how low-latitude magnetopause reconnection occurring for B_Y-dominated IMF ($B_Z \approx 0$, $B_Y \neq 0$) gives rise to a class of polar cap auroras known as bending arcs. We have now elucidated the dynamics during purely northward IMF, completing our understanding of the ECPC response of the magnetosphere to solar wind coupling under all IMF clock angle regimes.

There still remains much to understand. Several future studies are anticipated. We will investigate the clock angle range over which HCAs develop, to better understand the DLR process. We will study the temporal development of the HCA from the initial northward turning of the IMF to quantify the rate at which magnetic flux is closed by DLR. We will also use the evolution of the HCA to track the capture of solar wind plasma by the magnetosphere, its transport within the magnetosphere, and its link to the formation of the cold, dense plasma sheet.

Data Availability Statement

The OMNI data and the IMAGE WIC and SI12 data were obtained from CDAWeb (https://cdaweb.gsfc.nasa.gov). The DMSP/SSUSI file type EDR-AUR data were obtained from https://ssusi.jhuapl.edu (data version 0106, software version 7.0.0, calibration period version E0018). The DMSP/SSIES data were downloaded from the Madrigal Database at Millstone Hill (https://millstonehill.haystack.mit.edu). AMPERE data were obtained online (from https://ampere.jhuapl.edu).

References

Anderson, B. J., Takahashi, K., & Toth, B. A. (2000). Sensing global Birkeland currents with Iridium® engineering magnetometer data. *Geophysical Research Letters*, *27*(24), 4045–4048.

Axford, W. I., & Hines, C. O. (1961). A unifying theory of high-latitude geophysical phenomena and geomagnetic storms. *Canadian Journal of Physics*, *39*(10), 1433–1464.

Burch, J. L., Saflekos, N. A., Gurnett, D. A., Craven, J. D., & Frank, L. A. (1992). The quiet time polar cap: DE 1 observations and conceptual model. *Journal of Geophysical Research*, *97*(A12), 19,403–19,412.

Burke, W. J., Gussenhoven, M. S., Kelley, M. C., Hardy, D. A., & Rich, F. J. (1982). Electric and magnetic field characteristics of discrete arcs in the polar cap. *Journal of Geophysical Research*, *87*(A4), 2431–2443.

Carlson, H. C., & Cowley, S. W. H. (2005). Accelerated polar rain electrons as the source of sun-aligned arcs in the polar cap during northward interplanetary magnetic field conditions. *Journal of Geophysical Research*, *110*, A05302. https://doi.org/10.1029/2004JA010669

Carter, J. A., Milan, S. E., Fear, R. C., Kullen, A., & Hairston, M. R. (2015). Dayside reconnection under interplanetary magnetic field By-dominated conditions: The formation and movement of bending arcs. *Journal of Geophysical Research: Space Physics*, *120*, 2967–2978. https://doi.org/10.1002/2014JA020809

Carter, J. A., Milan, S. E., Fear, R. C., Walach, M.-T., Harrison, Z. A., Paxton, L. J., & Hubert, B. (2017). Transpolar arcs observed simultaneously in both hemispheres. *Journal of Geophysical Research: Space Physics*, *122*, 6107–6120. https://doi.org/10.1002/2016JA023830

Carter, J. A., Milan, S. E., Fogg, A. R., Paxton, L. J., & Anderson, B. J. (2018). The association of high-latitude dayside aurora with NBZ field-aligned currents. *Journal of Geophysical Research: Space Physics*, *123*, 3637–3645. https://doi.org/10.1029/2017JA025082

Carter, J. A., Milan, S. E., Fogg, A. R., Sangha, H., Lester, M., Paxton, L. J., & Anderson, B. J. (2020). The evolution of long-duration cusp spot emission during lobe reconnection with respect to field-aligned currents. *Journal of Geophysical Research: Space Physics*, *125*, e2020JA027922. https://doi.org/10.1029/2020JA027922

Chisham, G., Freeman, M. P., Coleman, I. J., Pinnock, M., Hairston, M. R., Lester, M., & Sofko, G. (2004). Measuring the dayside reconnection rate during an interval of due northward interplanetary magnetic field. *Annales Geophysicae*, *22*(12), 4243–4258.

Chisham, G., Lester, M., Milan, S. E., Freeman, M. P., Bristow, W. A., Grocott, A., et al. (2007). A decade of the Super Dual Auroral Radar Network (SuperDARN): Scientific achievements, new techniques and future directions. *Surveys in Geophysics*, *28*(1), 33–109.

Clauer, C. R., Xu, Z., Maimaiti, M., Ruohoneimi, J. M., Scales, W., Hartinger, M. D., et al. (2016). Investigation of a rare event where the polar ionospheric reverse convection potential does not saturate during a period of extreme northward IMF solar wind driving. *Journal of Geophysical Research: Space Physics*, *121*, 5422–5435. https://doi.org/10.1002/2016JA022557

Cowley, S. W. H. (1981). Magnetospheric and ionospheric flow and the interplanetary magnetic field. In *The Physical Basis of the Ionosphere in the Solar-Terrestrial System*, AGARD-CP-295, pp. (4–1)–(4–14).

Cowley, S. W. H., & Lockwood, M. (1992). Excitation and decay of solar wind-driven flows in the magnetosphere-ionosphere system. *Annales Geophysicae*, *10*, 103–115.

Coxon, J. C., Milan, S. E., & Anderson, B. J. (2018). A review of Birkeland current research using AMPERE. In *Electric currents in geospace and beyond, Geophysical Monograph Series* (Vol. *235*, pp. 257–278). https://doi.org/10.1002/9781119324522.ch16

Craven, J. D., Murphree, J. S., Frank, L. A., & Cogger, L. L. (1991). Simultaneous optical observations of transpolar arcs in the two polar caps. *Geophysical Research Letters*, *18*(12), 2297–2300.

Cumnock, J. A., & Blomberg, L. G. (2004). Transpolar arc evolution and associated potential patterns. *Annales Geophysicae*, *22*(4), 1213–1231.

Cumnock, J. A., Sharber, J. R., Heelis, R. A., Blomberg, L. G., Germany, G. A., Spann, J. F., & Coley, W. R. (2002). Interplanetary magnetic field control of theta aurora development. *Journal of Geophysical Research*, *107*(A7), 1108. https://doi.org/10.1029/2001JA009126

Dungey, J. W. (1961). Interplanetary magnetic field and the auroral zones. *Physical Review Letters*, *6*(2), 47.

Dungey, J. W. (1963). The structure of the exosphere, or adventures in velocity space. In C. Dewitt, J. Hieblot, & A. Lebeau (Eds.), *Geophysics: The Earth's Environment* (pp. 505–550). New York: Gordon and Breach.

Elphinstone, R. D., Murphree, J. S., Hearn, D. J., Heikkila, W., Henderson, M. G., Cogger, L. L., & Sandahl, I. (1993). The auroral distribution and its mapping according to substorm phase. *Journal of Atmospheric and Terrestrial Physics*, *55*(14), 1741–1762.

Fear, R. C., & Milan, S. E. (2012a). The IMF dependence of the local time of transpolar arcs: Implications for formation mechanism. *Journal of Geophysical Research*, *117*, A03213. https://doi.org/10.1029/2011JA017209

Fear, R. C., & Milan, S. E. (2012b). Ionospheric flows relating to transpolar arc formation. *Journal of Geophysical Research*, *117*, A09230. https://doi.org/10.1029/2012JA017830

Fear, R. C., Milan, S. E., Carter, J. A., & Maggiolo, R. (2015). The interaction between transpolar arcs and cusp spots. *Geophysical Research Letters*, *42*, 9685–9693. https://doi.org/10.1002/2015GL066194

Fear, R. C., Milan, S. E., Maggiolo, R., Fazakerley, A. N., Dandouras, I., & Mende, S. B. (2014). Direct observation of closed magnetic flux trapped in the high-latitude magnetosphere. *Science*, *346*(6216), 1506–1510.

Frank, L. A., Craven, J. D., Burch, J. L., & Winningham, J. D. (1982). Polar views of the Earth's aurora with Dynamics Explorer. *Geophysical Research Letters*, *9*(9), 1001–1004.

Frey, H. U. (2007). Localized aurora beyond the auroral oval. *Reviews of Geophysics*, *45*, RG1003. https://doi.org/10.1029/2005RG000174

Frey, H. U., Mende, S. B., Immel, T. J., Fuselier, S. A., Claflin, E. S., Gérard, J.-C., & Hubert, B. (2002). Proton aurora in the cusp. *Journal of Geophysical Research*, *107*(A7), 1091. https://doi.org/10.1029/2001JA900161

Fuselier, S. A., Dayeh, M. A., Livadiotis, G., McComas, D. J., Ogasawara, K., Valek, P., et al. (2015). Imaging the development of the cold dense plasma sheet. *Geophysical Research Letters*, *42*, 7867–7873. https://doi.org/10.1002/2015GL065716

Fuselier, S. A., Petrinec, S. M., Trattner, K. J., & Lavraud, B. (2014). Magnetic field topology for northward IMF reconnection: Ion observations. *Journal of Geophysical Research: Space Physics*, *119*, 9051–9071. https://doi.org/10.1002/2014JA020351

Goudarzi, A., Lester, M., Milan, S. E., & Frey, H. U. (2008). Multi-instrumentation observations of a transpolar arc in the northern hemisphere. *Annales Geophysicae*, *26*(1), 201–210.

Hardy, D. A., Burke, W. J., & Gussenhoven, M. S. (1982). DMSP optical and electron measurements in the vicinity of polar cap arcs. *Journal of Geophysical Research*, *87*(A4), 2413–2430.

Henderson, M. G., Murphree, J. S., & Weygand, J. M. (1996). Observations of auroral substorms occurring together with preexisting quiet time auroral patterns. *Journal of Geophysical Research*, *101*(A11), 24,621–24,640.

Hones, E. W. Jr., Craven, J. D., Frank, L. A., Evans, D. S., & Newell, P. T. (1989). The horse-collar aurora: A frequent pattern of the aurora in quiet times. *Geophysical Research Letters*, *16*(1), 37–40.

Hosokawa, K., Kullen, A., Milan, S., Reidy, J., Zou, Y., Frey, H. U., et al. (2020). Aurora in the polar cap: A review. *Space Science Reviews*, *216*(1), 15.

Iijima, T., & Potemra, T. A. (1976). The amplitude distribution of field-aligned currents at northern high latitudes observed by Triad. *Journal of Geophysical Research*, *81*(13), 2165–2174.

Imber, S. M., Milan, S. E., & Hubert, B. (2006). The auroral and ionospheric flow signatures of dual lobe reconnection. *Annales Geophyiscae*, *24*(11), 3115–3129.

Imber, S. M., Milan, S. E., & Hubert, B. (2007). Observations of significant flux closure by dual lobe reconnection. *Annales Geophysicae*, *25*, 1617–1627.

King, J. H., & Papitashvili, N. E. (2005). Solar wind spatial scales in and comparisons of hourly Wind and ACE plasma and magnetic field data. *Journal of Geophysical Research*, *110*, A02104. https://doi.org/10.1029/2004JA010649

Kullen, A., Brittnacher, M., Cumnock, J. A., & Blomberg, L. G. (2002). Solar wind dependence of the occurrence and motion of polar auroral arcs: A statistical study. *Journal of Geophysical Research*, *107*(A11), 1362. https://doi.org/10.1029/2002JA009245

Kullen, A., Fear, R. C., Milan, S. E., Carter, J. A., & Karlsson, T. (2015). The statistical difference between bending arcs and regular polar arcs. *Journal of Geophysical Research: Space Physics*, *120*, 10,443–10,465. https://doi.org/10.1002/2015JA021298

Lu, G., Li, W. H., Raeder, J., Deng, Y., Rich, F., Ober, D., et al. (2011). Reversed two-cell convection in the northern and southern hemispheres during northward interplanetary magnetic field. *Journal of Geophysical Research*, *116*, A12237. https://doi.org/10.1029/2011JA017043

Marcucci, M. F., Coco, I., Ambrosino, D., Amata, E., Milan, S. E., Bavassano Cattaneo, M. B., & Retinò, A. (2008). Extended SuperDARN and IMAGE observations for northward IMF: Evidence for dual lobe reconnection. *Journal of Geophysical Research*, *113*, A02204. https://doi.org/10.1029/2007JA012466

Mende, S. B., Heetderks, H., Frey, H. U., Lampton, M., Geller, S. P., Abiad, R., et al. (2000). Far ultraviolet imaging from the IMAGE spacecraft. 2. Wideband FUV imaging. *Space Science Reviews*, *91*, 271–285.

Mende, S. B., Heetderks, H., Frey, H. U., Lampton, M., Geller, S. P., Habraken, S., et al. (2000). Far ultraviolet imaging from the IMAGE spacecraft. 1. System design. *Space Science Reviews*, *91*(1–2), 243–270.

Mende, S. B., Heetderks, H., Frey, H. U., Stock, J. M., Lampton, M., Geller, S. P., et al. (2000). Far ultraviolet imaging from the image spacecraft. 3. Spectral imaging of Lyman-α and OI 135.6 nm. *Space Science Reviews*, *91*, 287–318.

Meng, C.-I. (1981). Polar cap arcs and the plasma sheet. *Geophysical Research Letters*, 8(3), 273–276.

Milan, S. E. (2015). Sun et lumière: Solar wind-magnetosphere coupling as deduced from ionospheric flows and polar auroras, *Magnetospheric Plasma Physics: The Impact of Jim Dungey's Research* (pp. 33–64). Cham: Springer.

Milan, S. E., Carter, J. A., & Hubert, B. (2020). Probing the magnetic structure of a pair of transpolar arcs with a solar wind pressure step. *Journal of Geophysical Research: Space Physics*, 125, e2019JA027196. https://doi.org/10.1029/2019JA027196

Milan, S. E., Hubert, B., & Grocott, A. (2005). Formation and motion of a transpolar arc in response to dayside and nightside reconnection. *Journal of Geophysical Research*, 110, A01212. https://doi.org/10.1029/2004JA010835

Milan, S. E., Lester, M., Cowley, S. W. H., & Brittnacher, M. (2000). Dayside convection and auroral morphology during an interval of northward interplanetary magnetic field. *Annales Geophysicae*, 18(4), 436–444.

Milan, S. E., Provan, G., & Hubert, B. (2007). Magnetic flux transport in the Dungey cycle: A survey of dayside and nightside reconnection rates. *Journal of Geophysical Research*, 112, A01209. https://doi.org/10.1029/2006JA011642

Murphree, J. S., Anger, C. D., & Cogger, L. L. (1982). The instantaneous relationship between polar cap and oval auroras at times of northward interplanetary magnetic field. *Canadian Journal of Physics*, 60(3), 349–356.

Newell, P. T., Liou, K., & Wilson, G. R. (2009). Polar cap particle precipitation and aurora: Review and commentary. *Journal of Atmospheric and Solar-Terrestrial Physics*, 71(2), 199–215.

Newell, P. T., & Meng, C.-I. (1995). Creation of theta-auroras: The isolation of plasma sheet fragments in the polar cap. *Science*, 270(5240), 1338–1341.

Øieroset, M., Raeder, J., Phan, T. D., Wing, S., McFadden, J. P., Li, W., et al. (2005). Global cooling and densification of the plasma sheet during an extended period of purely northward IMF on October 22–24, 2003. *Geophysical Research Letters*, 32, L12S07. https://doi.org/10.1029/2004GL021523

Østgaard, N., Mende, S. B., Frey, H. U., Frank, L. A., & Sigwarth, J. B. (2003). Observations of non-conjugate theta aurora. *Geophysical Research Letters*, 30(21), 2125. https://doi.org/10.1029/2003GL017914

Paxton, L. J., Meng, C.-I., Fountain, G. H., Ogorzalek, B. S., Darlington, E. H., Gary, S. A., et al. (1992). Special sensor ultraviolet spectrographic imager: An instrument description. In *Instrumentation for planetary and terrestrial atmospheric remote sensing* (Vol. 1745, pp. 2–15). International Society for Optics and Photonics.

Reidy, J. A., Fear, R. C., Whiter, D. K., Lanchester, B., Kavanagh, A. J., Milan, S. E., et al. (2018). Interhemispheric survey of polar cap aurora. *Journal of Geophysical Research: Space Physics*, 123, 7283–7306. https://doi.org/10.1029/2017JA025153

Reidy, J. A., Fear, R. C., Whiter, D. K., Lanchester, B. S., Kavanagh, A. J., Price, D. J., et al. (2020). Multiscale observation of two polar cap arcs occurring on different magnetic field topologies. *Journal of Geophysical Research: Space Physics*, 125, e2019JA027611. https://doi.org/10.1029/2019JA027611

Reiff, P. H. (1982). Sunward convection in both polar caps. *Journal of Geophysical Research*, 87(A8), 5976–5980.

Reiff, P. H., & Burch, J. L. (1985). IMF By-dependent plasma flow and Birkeland currents in the dayside magnetosphere: 2. A global model for northward and southward IMF. *Journal of Geophysical Research*, 90(A2), 1595–1609.

Rich, F. J., & Hairston, M. R. (1994). Large-scale convection patterns observed by DMSP. *Journal of Geophysical Research*, 99(A3), 3827–3844.

Sandholt, P. E., Farrugia, C. J., Cowley, S. W. H., Denig, W. F., Lester, M., Moen, J., & Lybekk, B. (1999). Capture of magnetosheath plasma by the magnetosphere during northward IMF. *Geophysical Research Letters*, 26(18), 2833–2836.

Scholer, M., & Treumann, R. A. (1997). The low-latitude boundary layer at the flanks of the magnetopause. *Space Science Reviews*, 80(1–2), 341–367.

Siscoe, G. L., & Huang, T. S. (1985). Polar cap inflation and deflation. *Journal of Geophysical Research*, 90(A1), 543–547.

Song, P., & Russell, C. T. (1992). Model of the formation of the low-latitude boundary layer for strongly northward interplanetary magnetic field. *Journal of Geophysical Research*, 97(A2), 1411–1420.

Taylor, M. G. G. T., Lavraud, B., Escoubet, C. P., Milan, S. E., Nykyri, K., Dunlop, M. W., et al. (2008). The plasma sheet and boundary layers under northward IMF: A multi-point and multi-instrument perspective. *Advances in Space Research*, 41(10), 1619–1629.

Terasawa, T., Fujimoto, M., Mukai, T., Shinohara, I., Saito, Y., Yamamoto, T., et al. (1997). Solar wind control of density and temperature in the near-earth plasma sheet: Wind/geotail collaboration. *Geophysical research letters*, 24(8), 935–938.

Valladares, C. E., Carlson Jr, H. C., & Fukui, K. (1994). Interplanetary magnetic field dependency of stable sun-aligned polar cap arcs. *Journal of Geophysical Research*, 99(A4), 6247–6272.

Waters, C. L., Anderson, B. J., & Liou, K. (2001). Estimation of global field aligned currents using the Iridium® system magnetometer data. *Geophysical Research Letters*, 28(11), 2165–2168.

Wing, S., Johnson, J. R., & Fujimoto, M. (2006). Timescale for the formation of the cold-dense plasma sheet: A case study. *Geophysical Research Letters*, 33, L23106. https://doi.org/10.1029/2006GL027110

Woch, J., & Lundin, R. (1992). Magnetosheath plasma precipitation in the polar cusp and its control by the interplanetary magnetic field. *Journal of Geophysical Research*, 97(A2), 1421–1430.

Zhang, Y., Paxton, L. J., Newell, P. T., & Meng, C.-I. (2009). Does the polar cap disappear under an extended strong northward IMF? *Journal of Atmospheric and Solar-Terrestrial Physics*, 71(17-18), 2006–2012.

Zhang, Y., Paxton, L. J., Zhang, Q.-H., & Xing, Z. (2016). Polar cap arcs: Sun-aligned or cusp-aligned? *Journal of Atmospheric and Solar-Terrestrial Physics*, 146, 123–128.

Zhang, Q.-H., Zhang, Y.-L., Wang, C., Lockwood, M., Yang, H.-G., Tang, B.-B., et al. (2020). Multiple transpolar auroral arcs reveal insight about coupling processes in the Earth's magnetotail. *Proceedings of the National Academy of Sciences*, 117(28), 16,193–16,198.

Zhu, L., Schunk, R. W., & Sojka, J. J. (1997). Polar cap arcs: A review. *Journal of Atmospheric and Solar-Terrestrial Physics*, 59(10), 1087–1126. https://doi.org/10.1016/S1364-6826(96)00113-7